

Temperature dependence of transverse- and longitudinal-optic modes in TiO₂ (rutile)

François Gervais and Bernard Piriou

*Centre de Recherches sur la Physique des Hautes Températures, Centre National de la Recherche Scientifique, 45045
Orléans Cedex, France*

(Received 26 February 1974)

The temperature dependence of the infrared reflectivity of rutile, TiO₂, is reported in the range 275–900 cm⁻¹ and from room temperature up to 1500 K, for both the A_{2u} - and E_u -type mode spectra. Reflectivity spectra are fitted with the aid of a four-parameter dispersion model based on the factorized form of the dielectric function. The equivalence between the classical dielectric response function and the phonon propagator provides a correlation between adjusted frequencies and damping and their quantum counterparts in terms of the phonon self-energy. The temperature dependence of the anharmonic frequency shift for the ferroelectric (FE) A_{2u} (TO) mode which has been shown to be linear in the vicinity of room temperature looks more rapid at high temperature. This may indicate the occurrence of an anharmonic coupling that involves the sixth-order Hamiltonian, which acts as a quadratic function of temperature to stabilize the FE mode together with quartic anharmonicity. The behavior of TO and LO phonon damping with increasing temperature shows that the phonon lifetimes in rutile are limited by anharmonic three-phonon coupling. Phonon lifetimes are found shorter than in other oxide crystals. Moreover, the ratio of the damping function evaluated at the harmonic frequency on the frequency of the A_{2u} (TO) mode is six times higher than the same ratio averaged on all other modes. Thus rather large anharmonicities are revealed in rutile that are correctly described by lowest-order terms in the phonon self-energy.

I. INTRODUCTION

Because of its scientific importance rutile, TiO₂, has been the subject of many experimental investigations. Though rutile is not a ferroelectric crystal, it is known^{1,2} that the frequency of the A_{2u} (TO) mode rapidly increases with increasing temperature, as in the case of ferroelectric crystals, thus involving a decrease of the static dielectric constant with increasing temperature. The dependence of the frequency of the A_{2u} (TO) mode on temperature has been experimentally investigated both by neutron scattering¹ and dielectric measurements² from room temperature down to 4 K. On the other hand, Samara and Peercy² have studied the temperature and pressure dependence of the Raman-active modes from 4 up to 500 K. These authors have found rather small self-energy shifts from the energy of the harmonic-vibration mode, while the self-energy of the so-called ferroelectric A_{2u} (TO) mode accounts for 20% of the vibration energy at 300 K. To make use of the Lyddane-Sachs-Teller relation, they have assumed that the A_{2u} (LO) mode frequency is temperature independent. The main conclusion was that, for the ferroelectric A_{2u} mode, the anharmonic frequency shift derived from the cubic Hamiltonian is counterbalanced by strong quartic anharmonicity which becomes predominant at temperatures higher than ~30 K, and which stabilizes the vibration mode. Such an effect has been predicted by Silverman and Joseph.³ Since the same situation occurs in many ferroelectric (FE) ma-

terials,⁴ it is of great interest to study this stabilization process. One of the authors has recently pointed out⁵ that to the same sixth order in the self-energy as the cubic term, the sixth-order Hamiltonian gives a contribution to the phonon self-energy the effect of which is also to stabilize the harmonic mode energy. However, while the temperature dependence of the quartic term is linear, it was pointed out that the lowest-order term involving the sixth-order Hamiltonian should involve a quadratic temperature dependence of the energy shift with the same positive sign. Thus it is of interest to study to what extent the data obtained by Samara *et al.*,² which show a linear behavior in the vicinity of room temperature, extrapolate up to high temperatures.

Since the A_{2u} mode is infrared active, measurements of the temperature dependence of infrared reflectivity should give information on the self-energy of this A_{2u} (TO) mode as well as on that of the corresponding LO mode. Also, to complete the study of the Raman-active modes by Samara *et al.*,² the anharmonic behavior of the infrared-active E_u modes will be presented in this paper.

To obtain as much information as possible from the infrared reflectivity spectra when the calculation of the dynamics of the anharmonic lattice would be of formidable complexity, a four-parameter dispersion model has been shown to be more suitable than the classical three-parameter model in the case of several polar-mode crystals having wide reflectivity bands.⁶ This four-parameter model has been tested for the E_u -type modes of

TiO₂ and Al₂O₃.⁶ In the case of only one reflectivity band and approximately for well-separated bands, it is straightforward to show that the classical dispersion model, as tested first by Spitzer and Kleinman⁷ in a crystal having many phonon branches such as α -quartz, implies equality for the longitudinal and transverse mode damping.⁶ When the reflectivity bands are narrow, as in quartz⁷ or silicates,^{8,9} it is reasonable to expect approximately the same phonon decay for the LO and the corresponding TO modes within the hypothesis of a two-phonon density of states which would be a slowly varying function of frequency. This is usually the case in crystals having a sufficient number of phonon branches regularly allocated in the Brillouin zone. On the other hand, when

$$\left| \frac{\Omega_{j\text{TO}}^2}{\Omega_{j\text{LO}}^2} - 1 \right| \gtrsim 1,$$

that is when the infrared band is wide, there is no reason for an identity between damping γ_{TO} and γ_{LO} because both phonon modes may have different phonon decays. Results obtained with the aid of the four-parameter model for the E_u modes in

$$H^{(n)} = \sum_{\vec{k}_1 j_1} \sum_{\vec{k}_2 j_2} \cdots \sum_{\vec{k}_n j_n} V^{(n)}(\vec{k}_1 j_1, \vec{k}_2 j_2, \dots, \vec{k}_n j_n) A(\vec{k}_1 j_1) A(\vec{k}_2 j_2) \cdots A(\vec{k}_n j_n). \quad (2)$$

The $V^{(n)}(\dots)$ potentials are Fourier-transformed n th-order atomic force constants¹⁰ and the operators $A(\vec{k}_i j_i)$ are defined in term of the usual phonon creation and annihilation operators

$$A(\vec{k}_i j_i) = a^\dagger(-\vec{k}_i j_i) + a(\vec{k}_i j_i). \quad (3)$$

The linear dielectric susceptibility tensor is defined as the analytic continuation of a sum of phonon propagators over all polar vibration modes and depends on a product of first-order dipolar-moment tensor components $M_{\mu j} M_{\nu j}$ associated with each polar phonon mode $(\vec{0}j)$,¹¹

$$\chi_{\mu\nu} = \frac{\beta}{v} \lim_{x \rightarrow 0} \sum_{\vec{0}j} M_{\mu j} M_{\nu j} G(\vec{0}j, \omega \pm ix, T), \quad (4)$$

where v is the volume of the crystal and $\beta = 1/k_B T$.

The phonon propagator may be evaluated by solving the Dyson equation within the approximation of assuming the self-energy matrix

$$P(\vec{0}j, \omega, T) = -\beta\hbar [\Delta\omega(\vec{0}j, \omega, T) \mp i\Gamma(\vec{0}j, \omega, T)] \quad (5)$$

as diagonal over the branch indices.^{10, 13} In Eq. (5), the real and imaginary parts of the phonon self-energy, respectively, correspond to the anharmonic frequency shift $\Delta\omega$ and the damping func-

tion Γ . If $\omega(\vec{0}j)$ is the harmonic frequency of a phonon mode, the phonon propagator that describes the spectral response of this phonon mode is¹⁰⁻¹²

$$G(\vec{0}j, \omega, T) = \frac{1}{\beta\hbar} \frac{2\omega(\vec{0}j)}{\omega^2(\vec{0}j) - \omega^2 - 2\omega(\vec{0}j)P(\vec{0}j, \omega, T)/\beta\hbar}. \quad (6)$$

We shall restrict ourselves and retain only the terms which contribute to the phonon self-energy up to the same order as the lowest-order contribution to the imaginary part of the self-energy, viz., the sixth. Within this approximation, three terms are known to contribute to the phonon self-energy. They are diagrammatically represented in Fig. 1. The first one [Fig. 1(a)] is due to the lowest-order effect of the quartic Hamiltonian. This term is real and thus only contributes to the frequency shift in the form^{10, 11}

$$\Delta\omega^{(4)}(\vec{0}j, T) = \frac{12}{\hbar} \sum_{\vec{k}_1 j_1} V^{(4)}(\vec{0}j, \vec{0}j, \vec{k}_1 j_1, -\vec{k}_1 j_1) [2n(\vec{k}_1 j_1) + 1], \quad (7)$$

where $n(\vec{k}_1 j_1) = (e^{n\omega(\vec{k}_1 j_1)/k_B T} - 1)^{-1}$ is the mean number of phonons, hereafter noted as n_1 .

$$\left| \frac{\Omega_{j\text{TO}}^2}{\Omega_{j\text{LO}}^2} - 1 \right| \ll 1,$$

whereas for the $E_u^{(3)}$ mode having the highest oscillator strength ($\Omega_{3\text{TO}} = 569 \text{ cm}^{-1}$, $\Omega_{3\text{LO}} = 909 \text{ cm}^{-1}$ at 300 K), it was verified that the imaginary part of the phonon self-energy increases monotonically from the value determined at $\omega = \Omega_{\text{TO}}$ up to another value at $\omega = \Omega_{\text{LO}}$, as may be expected.

II. PHONON SELF-ENERGY AND DIELECTRIC SUSCEPTIBILITY

In this section we review some fundamental expressions obtained by Maradudin and Fein,¹⁰ Cowley,¹¹ and one of the authors.⁵

By adopting the notation of Wallis *et al.*,¹² the anharmonic Hamiltonian may be expanded as

$$H_A = H^{(3)} + H^{(4)} + \cdots + H^{(n)} + \cdots, \quad (1)$$

where the n th-order Hamiltonian is

The second term [Fig. 1(b)] is due to the cubic Hamiltonian. Calculations by using the usual set of rules¹⁰ give the following contribution to the frequency shift and damping function:

$$\begin{aligned} \Delta\omega^{(6)}(\vec{0}j, \omega, T) + i\Gamma^{(6)}(\vec{0}j, \omega, T) = & -\frac{18}{\hbar^2} \sum_{\pm \vec{k}_1 j_1 j_2} |V^{(3)}(\vec{0}j, \vec{k}_1 j_1, -\vec{k}_1 j_2)|^2 \\ & \times \left\{ (n_1 + n_2 + 1) \left[\mathcal{P} \frac{1}{\omega + \omega_1 + \omega_2} + i\pi\delta(\omega + \omega_1 + \omega_2) - \mathcal{P} \frac{1}{\omega - \omega_1 - \omega_2} - i\pi\delta(\omega - \omega_1 - \omega_2) \right] \right. \\ & \left. + (n_2 - n_1) \left[\mathcal{P} \frac{1}{\omega + \omega_1 - \omega_2} + i\pi\delta(\omega + \omega_1 - \omega_2) - \mathcal{P} \frac{1}{\omega - \omega_1 + \omega_2} - i\pi\delta(\omega - \omega_1 + \omega_2) \right] \right\}, \end{aligned} \tag{8}$$

where, for simplicity, $\omega(\vec{k}_i j_i)$ is noted ω_i and \mathcal{P} denotes the principal part.

The third term [Fig. 1(c)] gives a real contribution as does the first. The result is⁵

$$\Delta\omega^{(6)}(\vec{0}j, T) = \frac{1440}{\beta \hbar^2} \sum_{\vec{k}_1 j_1, \vec{k}_2 j_2} V^{(6)}(\vec{0}j, \vec{0}j, \vec{k}_1 j_1, -\vec{k}_1 j_1, \vec{k}_2 j_2, -\vec{k}_2 j_2) \left[\frac{n_1 + n_2 + 1}{\omega_1 + \omega_2} - \frac{n_1 - n_2}{\omega_1 - \omega_2} \right]. \tag{9}$$

As long as the quartic potential is positive, as is apparently the case, the frequency shift $\Delta\omega^{(4)}(\vec{0}j, T)$ is positive, whereas $\Delta\omega^{(6)}(\vec{0}j, \omega, T)$ is usually negative in the vicinity of the normal-mode frequency.^{11,14} Thus both contributions balance each other. Within the hypothesis of a positive sign for the quartic potentials, the sixth-order potentials, which are second derivatives of the quartic potentials, are also positive. However, $\Delta\omega^{(6)}(\vec{0}j, T)$ is a quadratic function of temperature, whereas $\Delta\omega^{(4)}(\vec{0}j, T)$ and $\Delta\omega^{(6)}(\vec{0}j, \omega, T)$ vary linearly with increasing temperature in the high-temperature limit.

The linear dielectric susceptibility tensor is

$$\begin{aligned} \chi_{\mu\nu}(\omega, T) &= \chi'_{\mu\nu}(\omega, T) \pm i\chi''_{\mu\nu}(\omega, T) \\ &= \frac{1}{\hbar v} \sum_{\vec{0}j} M_{\mu j} M_{\nu j} \frac{2\omega(\vec{0}j)}{\omega^2(\vec{0}j) - \omega^2 + 2\omega(\vec{0}j)[\Delta\omega(\vec{0}j, \omega, T) \mp i\Gamma(\vec{0}j, \omega, T)]}. \end{aligned} \tag{10}$$

Within the lowest-order approximation, the damping $\Gamma(\vec{0}j, \omega, T)$ reduces to the imaginary part of Eq. (8),

$$\begin{aligned} \Gamma(\vec{0}j, \omega, T) &= \frac{18\pi}{\hbar^2} \sum_{\pm \vec{k}_1 j_1 j_2} |V^{(3)}(\vec{0}j, \vec{k}_1 j_1, -\vec{k}_1 j_2)|^2 \{ (n_1 + n_2 + 1)\delta(\omega - \omega_1 - \omega_2) \\ &+ (n_1 - n_2)[\delta(\omega + \omega_1 - \omega_2) - \delta(\omega - \omega_1 + \omega_2)] \}, \end{aligned} \tag{11}$$

while the frequency shift is the sum of terms $\Delta\omega^{(4)}(\vec{0}j, T)$, $\Delta\omega^{(6)}(\vec{0}j, T)$ added to the real part $\Delta\omega^{(6)}(\vec{0}j, \omega, T)$ of Eq. (8).

The form of Eq. (10) is that of the classical dielectric susceptibility

$$\chi = \chi' \pm i\chi'' = \sum_j \frac{\Delta\epsilon_j}{4\pi} \frac{\Omega_j^2}{\Omega_j^2 - \omega^2 \mp i\gamma_j\omega}, \tag{12}$$

where $\Delta\epsilon_j$ is the classical oscillator strength, and Ω_j and γ_j , respectively, are the resonance frequency and damping of a TO vibrational mode.

Equations (10) and (12) are equivalent when

$$(8\pi/\hbar v)\omega(\vec{0}j)M_{\mu j}M_{\nu j} \equiv \Omega_j^2 \Delta\epsilon_j, \tag{13}$$

$$\Omega_j^2 \equiv \omega^2(\vec{0}j) + 2\omega(\vec{0}j)\Delta\omega(\vec{0}j, \omega, T), \tag{14}$$

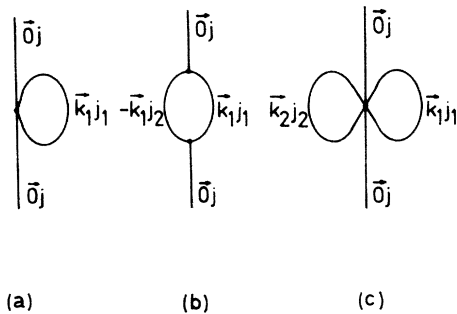


FIG. 1. Diagrams of the phonon-phonon interactions that contribute to the phonon self-energy up to the sixth order.

$$\omega\gamma_j \equiv 2\omega(\vec{0}j)\Gamma(\vec{0}j, \omega, T). \quad (15)$$

These equivalence relations imply a generalization of the classical dispersion formula (12) to take account of the possible frequency dependence of $\Delta\omega(\vec{0}j, \omega, T) + i\Gamma(\vec{0}j, \omega, T)$ and under these conditions either the classical or quantum forms of the dielectric susceptibility may be utilized.

III. FOUR-PARAMETER SEMIQUANTUM (FPSQ) MODEL

The form of the dielectric susceptibility (12) reflects the fact that the complex frequencies of the transverse-optic modes are the poles of the function χ and of the dielectric function

$$\epsilon = \epsilon_\infty + 4\pi\chi. \quad (16)$$

The complex frequencies of the longitudinal-optic modes are the zeros of the dielectric function and thus the poles of the function

$$\eta = 1/\epsilon. \quad (17)$$

Consequently, to obtain information on LO as well as on TO modes, it appears more suitable to use the factorized form of the dielectric function¹⁵

$$\begin{aligned} \epsilon &= \epsilon' \pm i\epsilon'' \\ &= \epsilon_\infty \prod_j \frac{\omega_{LO}^2(\vec{0}j) - \omega^2 + 2\omega_{LO}(\vec{0}j)[\Delta\omega_{LO}(\vec{0}j, \Omega_{jLO}, T) \mp i\omega\bar{\gamma}_{jLO}(T)]}{\omega_{TO}^2(\vec{0}j) - \omega^2 + 2\omega_{TO}(\vec{0}j)[\Delta\omega_{TO}(\vec{0}j, \Omega_{jTO}, T) \mp i\omega\bar{\gamma}_{jTO}(T)]}. \end{aligned} \quad (20)$$

This expression involves four adjustable parameters per polar phonon mode at each temperature, viz., $\Delta\omega_{TO}(\vec{0}j, \Omega_{jTO}, T)$, $\Delta\omega_{LO}(\vec{0}j, \Omega_{jLO}, T)$, $\bar{\gamma}_{jTO}(T)$, and $\bar{\gamma}_{jLO}(T)$. For the necessity of a first approach, Eq. (18) may be equivalently utilized when the harmonic frequencies (which will be determined by extrapolation down to $T=0$ of the frequency data) are unknown, and the four adjustable parameters are Ω_{jTO} , Ω_{jLO} , γ_{jTO} , and γ_{jLO} .

Infrared reflection spectra can be fitted with the aid of Eq. (18) or equivalently (20) together with

$$R = \left| \frac{\sqrt{\epsilon} - 1}{\sqrt{\epsilon} + 1} \right|^2. \quad (21)$$

Thus a measurement of the phonon self-energy at two frequencies, Ω_{TO} and Ω_{LO} , can be deduced from the infrared reflectivity data for each polar mode.

IV. EXPERIMENTAL PROCEDURE AND RESULTS

All infrared reflection spectra were measured with a single-beam Perkin-Elmer 12C mono-

$$\epsilon = \epsilon' \pm i\epsilon'' = \epsilon_\infty \prod_j \frac{\Omega_{jLO}^2 - \omega^2 \mp i\gamma_{jLO}\omega}{\Omega_{jTO}^2 - \omega^2 \mp i\gamma_{jTO}\omega}. \quad (18)$$

Tests of formula (18) in realistic cases⁶ have shown that the four parameters per polar mode may be considered as frequency independent, even in the case of wide reflectivity bands. Indeed, we make an approximation which holds as long as the structure of the crystal involves a sufficient number together with a regular frequency distribution of phonon branches in order that the two-phonon density of states (and *a fortiori* higher-order densities) would be a slowly varying function of frequency. Then $\Delta\omega^{(6)}(\vec{0}j, \omega, T)$ is assumed to be a constant, rewritten $\Delta\omega^{(6)}(\vec{0}j, \Omega_j, T)$, in the vicinity of the resonance frequency Ω_j , as are the two other contributions to the frequency shift. In view of relation (15), $\Gamma(\vec{0}j, \omega, T)$ should be of the form⁶

$$\Gamma(\vec{0}j, \omega, T) = \omega\bar{\gamma}_j(\omega, T). \quad (19)$$

A comparison of Eqs. (10) and (18) shows⁶ that the FPSQ model assumes a monotonic increase of the dimensionless damping function $\bar{\gamma}_j(\omega, T)$ from a value $\bar{\gamma}_{jTO}(T)$ at $\omega = \Omega_{TO}$ up to another value $\bar{\gamma}_{jLO}(T)$ at $\omega = \Omega_{LO}$, consistent with the above approximation. By making use of the equivalences (14) and (15) applied to the longitudinal modes, Eq. (18) may be rewritten in the form

chromator equipped with a sodium chloride or a cesium bromide prism. The average angle of the incident light beam was $7\frac{1}{2}^\circ$ from the normal to the sample surface. During the reflectivity measurements the infrared flux was chopped ahead of the sample so that the thermal radiation emitted by the crystal would appear as a constant flux and consequently was not detected. The thermal radiation emitted by the crystal at a minimum in the reflectivity may be compared to that emitted by the globar source heated at a known temperature, thus allowing the temperature measurement at the crystal surface seen by the entrance slit of the spectrometer. The chopper makes an angle with the infrared flux to avoid any reflection of the radiation emitted by the crystal into the spectrometer. The crystal is heated by a small electric furnace at temperatures lower than 800 K. Higher temperatures are obtained by heating by a CO_2 laser working in the continuous regime. Gervais¹⁶ has carefully verified by differential analysis that such a kind of heating by monochromatic radiation does not significantly disturb the normal phenom-

enon.

Optically polished rutile crystals were supplied by Hrand Djevahirdjian S.A. Crystals have been annealed for several hours at 1700 K so as to regenerate the surface after polishing. The uncertainty in the reflectivity is $\Delta R/R \approx 2\%$, to which one has to add an absolute uncertainty varying from $\Delta R = 0.002$ at 900 cm^{-1} to $\Delta R = 0.01$ at 300 cm^{-1} due to the noise in the detection. The resolution in the spectra is intermediate between 2 and 5 cm^{-1} .

Two crystals were employed. To get the A_{2u} -type vibration mode (extraordinary ray) one needs a gold-wire-grid polarizer together with a crystal cut parallel to the \vec{c} axis, whereas a surface cut perpendicular to the \vec{c} axis readily reflects the E_u -type mode spectrum (ordinary ray). Spectra obtained at room temperature are shown in Figs. 2 and 3. Comparison of these spectra with those obtained by Spitzer *et al.*¹⁷ shows agreement within experimental error except in the range $500\text{--}600 \text{ cm}^{-1}$ for the ordinary ray (Fig. 3), where our data are slightly lower than those of Spitzer *et al.* A small dip appears in this frequency range in both spectra that is not expected from group-theory analysis ($1A_{2u} + 3E_u$ infrared-active modes). The same dip is noted in the spectra obtained by Spitzer *et al.*¹⁷ but looks less marked in the spectra of Barker and Tinkham.¹⁸ Thus we think the small disagreement in Fig. 3 between our data and those of Spitzer *et al.* is correlated to the intensity of the dip that seems to vary from one spectrum to another. The cause of this feature will be discussed in Sec. V.

Results at several temperatures are shown in Figs. 4, 7, and 8.

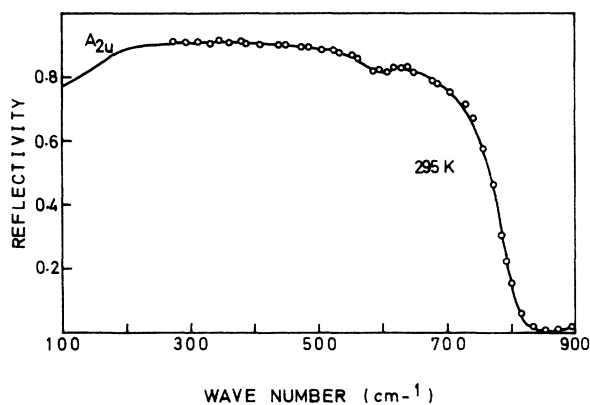


FIG. 2. Reflectivity data (open circles) for the A_{2u} -type mode spectrum at room temperature, and the best fit (full curve) to these data with the aid of the four-parameter dispersion model.

V. ANALYSIS OF THE DATA

A. A_{2u} -type mode at room temperature

To fit the A_{2u} mode spectrum, which is incomplete in the low frequencies owing to the limit in the available spectral range of our apparatus, one needs an additional parameter, viz., the frequency of the TO mode. We have used² that determined by neutron scattering measurements,¹ $\Omega_{\text{TO}} = 172 \text{ cm}^{-1}$. A secondary oscillator near 600 cm^{-1} has been added to take account of the marked dip. Then a fit of Eq. (18) to the reflectivity data looks excellent since it is within experimental error (Fig. 2). Parameters used for the best fit are listed in Table I.

The good agreement between the calculated curve and experimental data tends to indicate that the approximations made are valid. Particularly, any peak in the damping function would be observed in the range $280\text{--}550 \text{ cm}^{-1}$ as a slight local disagreement in the fit.

It is possible that the additional oscillator near 600 cm^{-1} is a two-phonon absorption. Two-phonon peaks indeed are observed in Raman spectra^{2,19} and a high phonon density does exist in the Brillouin-zone boundaries at energies equal to about half that of the secondary oscillator, particularly at the X and M points.¹ But this secondary oscillator may be alternatively understood in term of a forbidden mode, since the oscillator frequency differs by only 3% from that of the A_{1g} -type mode which is known to be strong in the Raman spectrum.^{2,19} Indeed, the existence of a

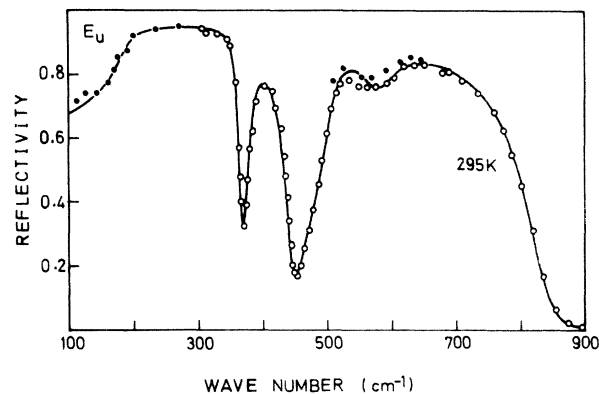


FIG. 3. Reflectivity data (open circles) for the E_u mode spectrum at room temperature. The data obtained by Spitzer *et al.* (Ref. 17) have been added (full circles in the range $500\text{--}600 \text{ cm}^{-1}$) when they differ from ours. They complete our data in the low-frequency range. The full curve is the best fit of Eq. (18) to the data.

TABLE I. Temperature dependences of frequencies, frequency shifts, and damping of the A_{2u} -type mode spectrum as obtained from the best fit to the reflectivity data.

Mode	T	Ω_j (cm^{-1})	$\Delta\omega(\vec{0}j, \Omega_j, T)$ (cm^{-1})	$\Delta\omega(\vec{0}j, \Omega_j, T) + \delta\omega_j$ (cm^{-1})	γ_j (cm^{-1})	$\Gamma(\vec{0}j, \Omega_j, T)$ (cm^{-1})		
A_{2u} TO	T_1	142 ^[2]	-2 ^[2]	-2 ^[2]	$\omega_{\text{TO}} = 144 \text{ cm}^{-1}$ ^[2]	
	T_2	172 ^[1]	36 ^[2]	31 ^[2]	(76)	(45.4)		
	T_3	(191)		(55)	131	90.5		
	T_4	(212)		(85)	158	117		
	T_5	(250)		(145)	169	147		
	T_6	275	226	190	178	170		
LO	T_2	796			38	19		
	T_3	798			60	30		
	T_4	798			90	45		
	T_5	794			135	67		
	T_6	788			157	78		
$\epsilon_\infty = 7.8$								
		$\Omega_{j\text{TO}}$ (cm^{-1})	$\Omega_{j\text{LO}}$ (cm^{-1})	$\gamma_{j\text{TO}} = \gamma_{j\text{LO}}$ (cm^{-1})				
secondary mode	T_2	592	589.5	55				
	T_3	592	587	80				
	T_4	588	582	110				
	T_5	580	571.5	(135)				
	T_6	570	559	(150)				
$T_1 = 4 \text{ K}, T_2 = 295 \text{ K}, T_3 = 563 \text{ K}, T_4 = 840 \text{ K}, T_5 = 1285 \text{ K}, T_6 = 1550 \text{ K}$								

small amount of a (3+) impurity such as Fe^{3+} , substituted on a Ti^{4+} site, locally removes the neutrality of charges in the A_{1g} vibration mode, thus giving a slight polar character to the mode. This reasoning is compatible both with the amount of (3+) impurity in our sample and with the slight change in the intensities of the dip observed by different authors, since impurities may vary from one crystal to another.

Finally it is possible that the addition of both effects creates the dip near 600 cm^{-1} . These arguments also hold for the pronounced dip observed in the same frequency range in the E_u spectrum (Fig. 3).

B. E_u -type modes at several temperatures

There is no problem in fitting the E_u spectrum at room temperature since our data which extend from the high-frequency side down to 300 cm^{-1} may be completed by those obtained at still lower frequencies by Spitzer *et al.*¹⁷ in agreement with neutron scattering result¹ (Fig. 3). The dip near 600 cm^{-1} is treated again as a secondary oscillator. Results from the best fit are listed in Table II. A comparison of the TO and LO frequencies with those determined by neutron scattering measurements shows reasonable agreement within uncertainties due to experimental errors inherent to

TABLE II. Frequencies and damping of the E_u -type modes as deduced from the best fit to the reflectivity data as a function of temperature.

Mode	j	T	Transverse mode		Longitudinal mode		
			$\Omega_{j\text{TO}}$ (cm^{-1})	$\gamma_{j\text{TO}}$ (cm^{-1})	$\Omega_{j\text{LO}}$ (cm^{-1})	$\gamma_{j\text{LO}}$ (cm^{-1})	
E_u	1	T_1	189	27	831	50	
		T_2	(201)	43	831	65	
		T_3	(208)	54	831	86	
		T_4	(215)	82	828	115	
		T_5	(218)	95	826	145	
	2	T_1	381.5	16.5	367	10	
		T_2	377.5	27	364.5	16	
		T_3	374	33	363	23	
		T_4	362.5	50	356.5	35	
		T_5	355	60	353	47	
	3	T_1	508	24	443.5	21.5	
		T_2	502	38	439	33	
		T_3	501	52	433	42	
		T_4	496	87	424	67	
		T_5	492	110	415	76	
secondary mode	T_1	585	65	575	65		
	T_2	585	75	573	75		
	T_3	585	100	573	100		
	T_4	580	120	563	120		
	T_5	580	140	560	140		
$\epsilon_\infty = 6$							
$T_1 = 295 \text{ K}, T_2 = 535 \text{ K}, T_3 = 740 \text{ K}, T_4 = 1170 \text{ K}, T_5 = 1475 \text{ K}$							

TABLE III. Comparison of existing frequency data obtained by neutron scattering (Ref. 1) at room temperature with our data.

Mode	Neutron determination (cm ⁻¹)	Our data (FPSQ-model fit) (cm ⁻¹)
A_{2u} (TO)	172	...
$E_u^{(1)}$ (TO)	189	189 ^a
$E_u^{(2)}$ (LO)	375	367
$E_u^{(2)}$ (TO)	...	381.5
$E_u^{(3)}$ (LO)	429	443.5
$E_u^{(3)}$ (TO)	495	508
A_{2u} (LO)	...	796
$E_u^{(1)}$ (LO)	845	831

^a Deduced from a fit to the data of Spitzer *et al.* (Ref. 17) with the aid of the FPSQ model.

both techniques and to the simplicity of the model used to fit the data (Table III).

Fifteen among the sixteen parameters that formula (18) requires to fit the ordinary ray at higher temperatures are unambiguously imposed by the experimental results. Indeed the TO and LO frequencies are approximately positioned at the highest-slope points in the reflectivity band edges while damping determines the slope of the curve at these points. Besides, for wide bands, it is well known that damping is connected to the difference between the reflectivity maximum and unity. Also when the TO frequency of a weak polar mode (such as $E_u^{(2)}$ or $E_u^{(3)}$) is located between the TO and LO frequencies of a strong mode to which a large TO/LO splitting thus corresponds ($E_u^{(1)}$ mode), the lifetime of the weak phonon mode de-

termines the depth of the resulting dip in the main wide reflectivity band. It is known that the static dielectric constant ϵ_a (Ref. 2) decreases with increasing temperature according to a modified Curie-Weiss law. Thus we have estimated the frequency of the $E_u^{(1)}$ (TO) mode at several temperatures from the ϵ_a values calculated by using parameters given in Ref. 2 and with the aid of a generalized Lyddane-Sachs-Teller relation [by putting $\omega = 0$ in Eq. (18)]. The result is a hardening of the $E_u^{(1)}$ (TO) mode with increasing temperature.

Because of the simplicity of the model together with the relatively large spectral range where each parameter locally influences reflectivity, one obtains a single set of parameters (Table II) that permits the best fit to the experimental data at several temperatures (Fig. 4).

It is to be noted that Kramers-Kronig analysis is incorrect as long as the reflectivity spectrum is not known in the whole spectral range.

The imaginary parts of the dielectric functions ϵ and η have been calculated by using parameters given in Table II, at room and high temperatures (Fig. 5).

VI. SELF-ENERGY OF THE TO (FE) AND LO A_{2u} MODES

A. Frequency shift

Results obtained from dielectric measurements^{2,20} show that the real part of the phonon self-energy of the A_{2u} (TO) mode amounts to $\sim 20\%$ of the phonon energy at 300 K. Thus an estimation of the shift of frequency as made for the $E_u^{(1)}$ (TO) mode is no longer valid for this mode.

In addition to the anharmonic frequency shift, it is well known that the thermal lattice expansion creates a frequency shift

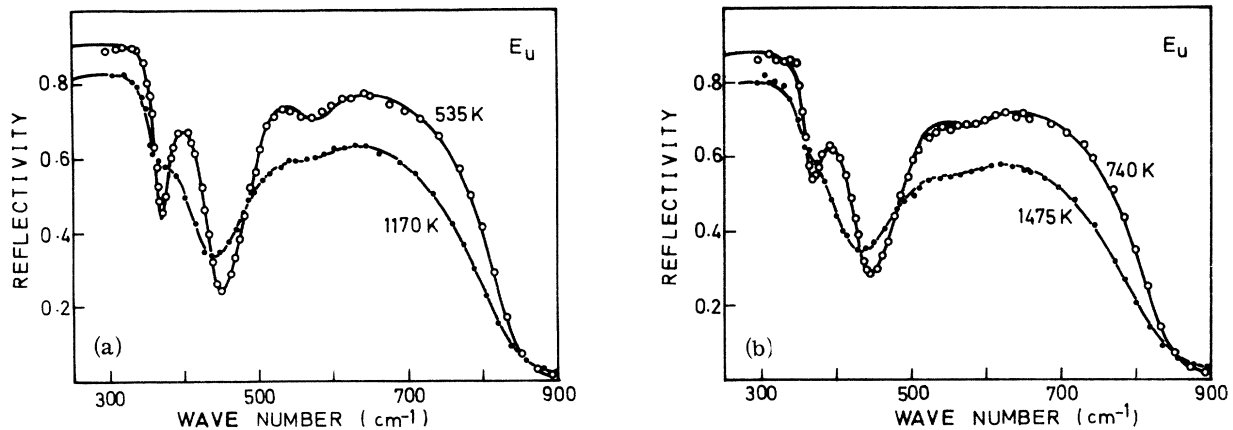


FIG. 4. Temperature dependence of reflectivity for the E_u mode spectrum. Best fits (full curves) to these data with the aid of the four-parameter model.

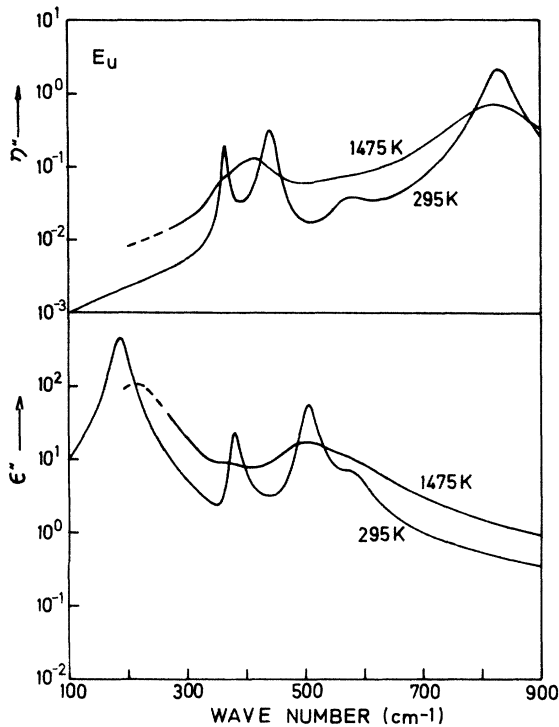


FIG. 5. Imaginary dielectric functions ϵ'' and η'' showing the change in the E_u -type mode structure with increasing temperature.

$$\delta\omega_j(T) = -\omega(\vec{0}j) \int_0^T g_j(T) \alpha_v(T) dT, \quad (22)$$

where g_j is the mode Grüneisen parameter and α_v the volume expansion coefficient. The func-

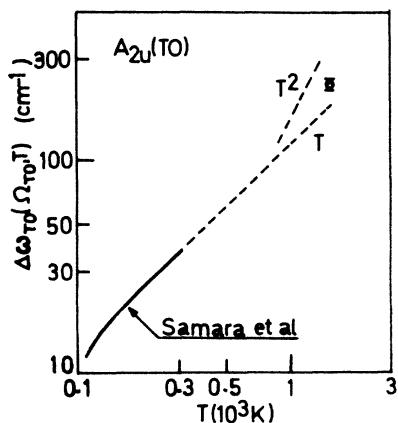


FIG. 6. Temperature dependence of the anharmonic frequency shift of the FE $A_{2u}(\text{TO})$ mode (full line) as obtained by Samara and Peercy (Ref. 2) and the extrapolation up to 1550 K of these data (dashed line). The anharmonic frequency shift deduced from the fit of the reflectivity at 1550 K appears higher (open circle) than the extrapolated value.

tions $g_j(T)$ and $\delta\omega_j(T)$ are known² between 4 and 300 K for the $A_{2u}(\text{TO})$ mode, together with the anharmonic frequency shift $\Delta\omega_{\text{TO}}(\vec{0}j, \Omega_{j\text{TO}}, T)$.

The first approach we have employed to fit the spectrum obtained at 1550 K was to use the value²¹

$$\Omega_{\text{TO}} = [\omega_{\text{TO}}^2 + 2\omega_{\text{TO}}(\Delta\omega_{\text{TO}} + \delta\omega_{\text{TO}})]^{1/2}$$

calculated at 1550 K by using an anharmonic shift $\Delta\omega_{\text{TO}}$ and a pure-volume effect $\delta\omega_{\text{TO}}$ deduced from a linear extrapolation up to 1550 K (Fig. 6) of existing data² which indeed exhibit a linear behavior in the range 150–300 K. The best fit to the reflectivity data by using such a value, viz., $\Omega_{\text{TO}} = 250 \text{ cm}^{-1}$, departs from the experimental points in the range 275–300 cm^{-1} (Fig. 7, dashed line). A better fit is achieved by using a value for Ω_{TO} equal at least to 275 cm^{-1} (Fig. 7, full line). This determination should be regarded with some caution because the accuracy of the reflectivity data decreases by approaching the low-frequency limit available with our apparatus. Nevertheless, since the reflectivity data keep a constant level at lower temperatures (Figs. 2 and 8), we think the slight decrease in the reflectivity observed at high temperature on the low-frequency side is effective. Besides the uncertainty has been lowered by performing high-temperature experiments for several times and by taking the average of the results.

If then one admits that the shift $\delta\omega_{\text{TO}}$ remains linear at temperatures higher than 300 K, the anharmonic frequency shift exhibits an increase with temperature which is more rapid than a linear one, since the result found at 1550 K is 40 cm^{-1} higher than the linearly extrapolated value. This behavior may be explained in terms of a contribution to the phonon self-energy due to the process

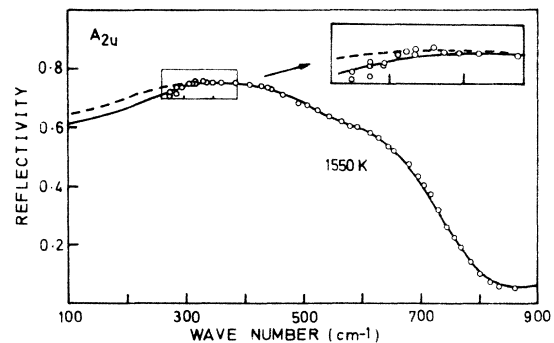


FIG. 7. Reflectivity data (open circles) for the A_{2u} mode at 1550 K. The best fit to these data by imposing the TO frequency 250 cm^{-1} deduced from the extrapolation of existing data (Ref. 2) (dashed curve) departs from the observed results in the low-frequency range. A better fit (full curve) is achieved by using a TO frequency equal to 275 cm^{-1} .

represented in the diagram of Fig. 1(c), since the corresponding term [Eq. (9)], which is expected positive, has a quadratic temperature dependence in the high-temperature limit, whereas the two other terms have a linear dependence. The effect of this kind of anharmonic interaction might be even more pronounced than is apparent in this result. Formally, higher-order quartic anharmonic terms¹² might indeed give a negative contribution to the frequency shift that would balance a part of the contribution of term $\Delta\omega^{(6)}(\vec{0}j, T)$. But since higher-order terms do not contribute to the damping function as we shall see below, there exists little support to this latest speculation. Thus our experiment indicates the contribution of an anharmonic coupling which involves the sixth-order Hamiltonian, together with the effect of the quartic Hamiltonian to the lowest order. Both anharmonic effects stabilize the vibrational motion of the ferroelectric TO mode at high temperature.

The values of Ω_{TO} at intermediate temperatures have been determined by interpolation of data found at 300² and 1500 K. On this basis one obtains good fits to the reflectivity data as shown in Fig. 8. The change in the phonon mode structure at high temperature with respect to that at room temperature is shown in Fig. 9. The imaginary parts of the dielectric functions ϵ and η have been calculated by using parameters given in Table I.

Since the pressure dependence of frequency Ω_{LO} is not available for now, it is not possible to separate the pure-volume effect from the anharmonic contribution to the shift of the LO mode. We note the weakness of the shift even over a wide range of temperatures since it does not exceed 1.25% up to 1550 K. There are two main ways to explain this result. First a negative Grüneisen mode pa-

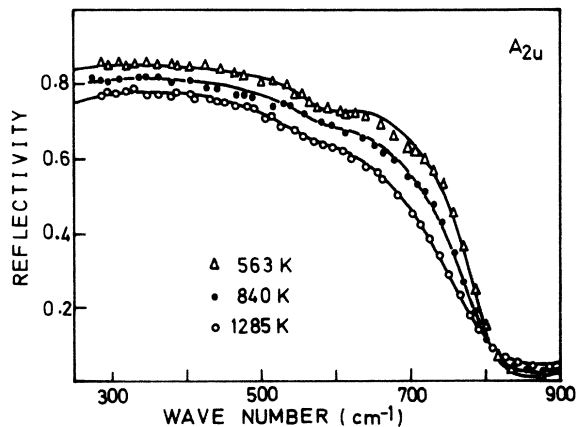


FIG. 8. Temperature dependence of the reflectivity (symbols) for the A_{2u} mode and the best fits (full curves) of Eq. (18) to these data.

rameter would cause a shift of frequency which might counterbalance the usual cubic anharmonic shift, as observed for the B_{1g} Raman-active mode,² or negative and positive contributions to the real part of the phonon self-energy expressed through the terms $\Delta\omega^{(6)}(\vec{0}j, \Omega_{\text{LO}}, T)$ and $\Delta\omega^{(4)}(\vec{0}j, T)$ balance each other.²² Finally it is to be noted parenthetically that the approximation made by Samara *et al.* [Eqs. (4) and (5) of Ref. 2] appears quite valid; that is, the observed frequency of the LO mode may be regarded as nearly temperature independent.

B. Phonon lifetime

One may generally consider that summation processes in Eq. (11) dominate difference processes at frequencies equal or higher than the TO frequency, to which the top of the reflectivity band corresponds. This is verified by recent calculations.²³ Difference processes may be neglected *a fortiori* in the relaxation of the LO modes. Thus, according to a procedure commonly used,^{8,9,24} we neglect the difference processes and introduce the frequency $\Omega_j/2$ that is the average frequency of the phonons interacting with the studied phonon ($\vec{0}j$) so that Eq. (11) may be simplified and rewritten in the form

$$[\Gamma(\vec{0}j, \omega, T)]_{\omega=\Omega_j} = \frac{1}{2} a_j [(e^{h\Omega_j(T)/2k_B T} - 1)^{-1} + \frac{1}{2}], \quad (23)$$

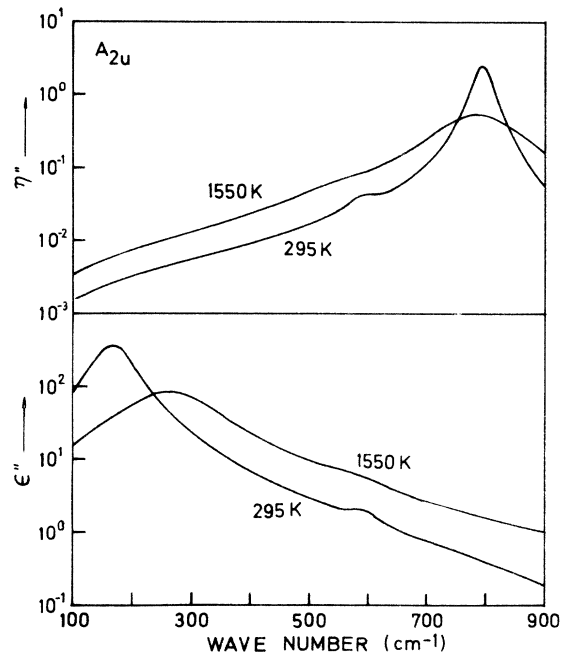


FIG. 9. Structures of the TO and LO A_{2u} modes at two temperatures. Imaginary dielectric functions are calculated by using parameters listed in Table I.

where a_j may be called the cubic anharmonic parameter, equal to $4\Gamma^{(6)}(\vec{0}_j, \Omega_j, 0)$ by putting $T=0$ in Eq. (23).

$\Gamma(\vec{0}_j, \Omega_j, T)$ has been evaluated at several temperatures from the damping data of the TO mode (Table I) and also from the width at half height of the neutron peak at 50 and 300 K,¹ by making use of the equivalence relation (15) at $\omega = \Omega_j$:

$$\left[\frac{\Gamma(\vec{0}_j, \omega, T)}{\omega} \right]_{\omega = \Omega_j} = \frac{\gamma_j}{2\omega(\vec{0}_j)}. \quad (24)$$

A fit of Eq. (23) to these data as a function of temperature by adjusting the parameter a_j only gives good agreement apart from the neutron value at 300 K (Fig. 10) and allows one to conclude that the TO-phonon lifetime is essentially limited by anharmonic three-phonon coupling. A fit of Eq. (23) to the LO damping data (Table I) also shows good agreement (Fig. 10), thus allowing the same conclusion. Higher-order anharmonic terms^{5, 12} indeed would involve a T^α temperature dependence in the high-temperature limit with α higher than 1.

The unusual shape (less than linear in the high-temperature limit) of the curve $\Gamma_{TO}(T)$ in a log-log scale is to be noted (Fig. 10), owing to the large increase of the Ω_{TO} frequency with increasing temperature. The success of the fit here gives an ad-

ditional argument to indicate the hardening of the transverse mode with increasing temperature.

Thus the anharmonic behavior of the TO and LO A_{2u} modes is correctly described by retaining terms up to the sixth order in the phonon self-energy only.

VII. TEMPERATURE DEPENDENCE OF E_u -TYPE MODE DAMPING

In the absence of any value of the mode Grüneisen parameters, the effect $\delta\omega_j$ of thermal lattice expansion is unknown and consequently the real part of the self-energy cannot be evaluated. However, since the frequencies are linearly shifted with increasing temperature, one can say that cubic anharmonicity together with thermal expansion effects are dominant processes for all modes, apart from the $E_u^{(1)}$ (TO) mode which looks stabilized by quartic anharmonicity, but to a lower extent than the ferroelectric A_{2u} (TO) mode.

The shifts of frequency from 300 to 1500 K are small enough for the E_u -type modes in order that $\Gamma(\vec{0}_j, \Omega_j, T)$ may be replaced by $\gamma_j/2$ in Eq. (23) apart from the $E_u^{(1)}$ (TO) mode for which the transformation, Eq. (24), has been made.

Reasonably good fits of Eq. (23) to the TO and LO damping data are achieved (Fig. 11–13) and one may conclude that anharmonic terms of higher order than the cubic one do not contribute to limit the phonon lifetime.

The fact that γ_{2LO} is significantly different from γ_{2TO} for the $E_u^{(2)}$ mode, where the splitting TO/LO is weak (Table 2, Fig. 12), together with imperfections in the fit of the infrared reflectivity in the vicinity of the TO frequency of mode $E_u^{(3)}$ at room temperature (Fig. 2), indicates that the use of the FPSQ dispersion model to treat the case of

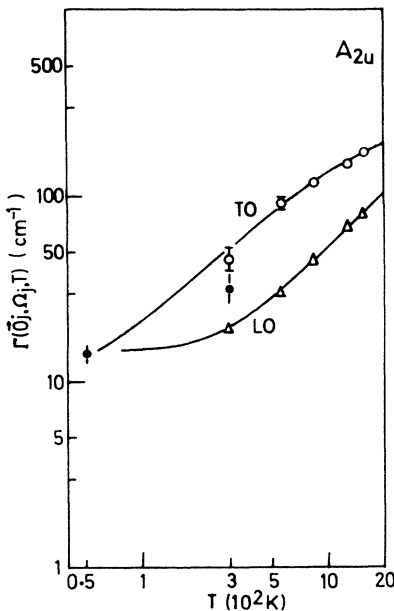


FIG. 10. Temperature dependence of the quantum damping function averaged in the vicinity of the resonance frequency for the TO (open circles) and LO (triangles) A_{2u} -type modes. The width at half-height of the neutron peaks for the transverse mode from Ref. 1 have been added after transformation according to Eq. (15) (full circles). Full curves are fits of Eq. (23) to these data.

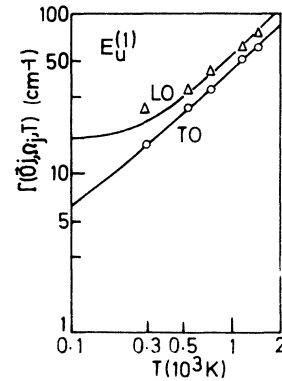


FIG. 11. Calculated curves [Eq. (23)] of the quantum damping function averaged in the vicinity of the resonance frequency (full curves) compared to the observed values (symbols) for the TO and LO $E_u^{(1)}$ -type modes as a function of temperature.

rutile lies at the limit of validity in some respects. It is apparent from the results for the $E_u^{(2)}$ mode that the function $\bar{\gamma}_2(\omega, T)$ is a rapidly varying function of frequency, contrary to the assumptions of the model. Nevertheless, the actual form of $\bar{\gamma}_2(\omega, T)$ probably does not depart significantly from a monotonic change from $\bar{\gamma}_{2LO}$ up to $\bar{\gamma}_{2TO}$ in the range $\Omega_{2LO} \rightarrow \Omega_{2TO}$ as assumed by the model,⁶ since the fit to the reflectivity data is good. The utilization of a frequency-dependent function for $\bar{\gamma}_{3TO}$ and $\bar{\gamma}_{3LO}$ would improve the fit in the range 500–600 cm^{-1} . But it is to be emphasized that the addition of other adjustable parameters tends to involve several solutions to a fit problem whereas the sets of parameters found to obtain the best fit to the present reflectivity curves are unique as long as one uses the FPSQ model.

VIII. POLAR CHARACTER OF THE MODES

When the polarization of the electromagnetic radiation implies the infrared activity of only one optic mode, as is the case for the A_{2u} -type mode, the equivalence of the real part of Eq. (18) for $j=1$ and the real classical dielectric function

$$\epsilon' = \epsilon_\infty + \Delta\epsilon \frac{\Omega_{TO}^2 (\Omega_{TO}^2 - \omega^2)}{(\Omega_{TO}^2 - \omega^2)^2 + \gamma_{TO}^2 \omega^2} \quad (25)$$

gives the following relation

$$\frac{\Delta\epsilon}{\epsilon_\infty} = \frac{\Omega_{LO}^2 - \Omega_{TO}^2}{\Omega_{TO}^2} \quad (26)$$

The substitution of Eq. (13) into formula (26) yields

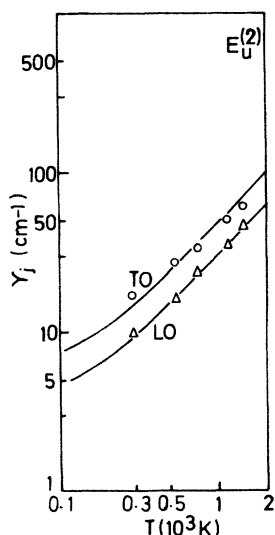


FIG. 12. Best fit of Eq. (23) to the TO and LO damping data of the $E_u^{(2)}$ mode.

$$M_\mu M_\nu = \frac{\epsilon_\infty \hbar \nu}{8\pi} \frac{\Omega_{LO}^2 - \Omega_{TO}^2}{\omega_{TO}} \quad (27)$$

Thus in terms of the usual classical dispersion theory, the rapid increase of the A_{2u} (TO) mode frequency with increasing temperature, while Ω_{LO} remains nearly a constant in Eq. (26), causes a large decrease of the classical oscillator strength $\Delta\epsilon$ from 160 at 300 K down to 56 at 1550 K. Apparently this would mean that the A_{2u} mode loses its polar character. Actually if one makes use of the quantum-theory results, Eq. (27) indicates that the product of dipolar-moment components $M_\mu M_\nu$ decreases by less than 10% when the temperature changes from 300 up to 1550 K and thus the polar character is nearly conserved in spite of the hardening of the TO mode.

The same consideration also holds for the polar characters of the $E_u^{(1)}$ and $E_u^{(3)}$ modes as well, since the products $M_{\mu j} M_{\nu j}$ look nearly temperature independent.

However this is not verified for the $E_u^{(2)}$ mode, where the TO/LO splitting diminishes markedly (Fig. 14) and thus the mode loses its polar character with increasing temperature. $M_{\mu 2} M_{\nu 2}$ (also $\Delta\epsilon_2$) is reduced indeed by a factor ≈ 5 when the temperature increases from room temperature up to 1500 K.

A temperature dependence of a dipolar-moment component $M_{\lambda j}$ in Eq. (4) is inconsistent with the usual quantum theory of the linear dielectric susceptibility and necessitates a renormalization of the dipolar moment as a result of the change of the relative positions of the ions during the thermal lattice expansion. This problem of renormal-

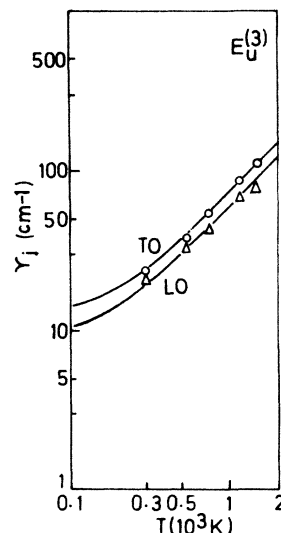


FIG. 13. Best fit of Eq. (23) to the TO and LO damping data of the $E_u^{(3)}$ mode.

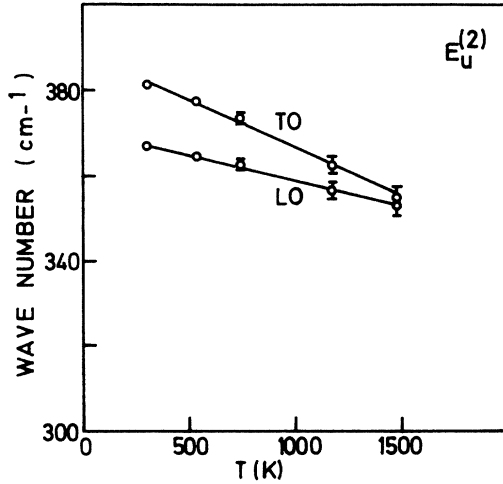


FIG. 14. Temperature dependence of the TO and LO frequencies of the $E_u^{(2)}$ -type mode. The mode loses its polar character since the TO/LO splitting diminishes with increasing temperature.

ization is removed by using the factorized form (18) of the dielectric function since the dipolar-moment components do not enter the function explicitly.

IX. DISCUSSION AND CONCLUSION

Though the FPSQ dispersion model is simplified with respect to quantum theory, since the actual frequency dependence of the cubic anharmonicity [Eq. (8)] is neglected (though partly taken into account since it is measured at two frequencies per polar mode) to retain the temperature dependence only, this model has allowed us to obtain information concerning the phonon self-energy in rutile crystal.

First, cubic anharmonicity alone limits the phonon lifetimes in the whole temperature range. The strength of this anharmonic coupling is measured through the parameter a_j . The ratio $a_j/\omega(\vec{0}_j)$ is a dimensionless number which is a characteristic of the summation over j phonon branches and \vec{k} wave-vector space of the cubic potentials in Eq. (11) and thus corresponds to a kind of two-phonon summation density of states. Results found in rutile may be compared (Table IV) to that found in other oxide crystals having several polar phonon modes such as corundum Al_2O_3 (Ref. 6) or the most simple of silicate crystals, viz., zircon ZrSiO_4 .⁹ Cubic anharmonicity appears large in rutile in comparison to other crystals owing to the value ~ 0.050 for the average ratio $a_j/\omega(\vec{0}_j)$ for the E_u -type modes in this crystal. Furthermore $a_j/\omega(\vec{0}_j)$ is found equal to 0.30 for the $A_{2u}(\text{TO})$ mode (Table IV). Taking account of the

TABLE IV. Comparison of the cubic anharmonic parameter and the ratio $a_j/\omega(\vec{0}_j)$ for the TO and LO modes in rutile with data found in two other crystals.

	Mode	Ω_j (at 300 K) (cm^{-1})	a_j (cm^{-1})	$a_j/\omega(\vec{0}_j)$
TiO ₂	$A_{2u}(\text{TO})$	172	43	0.30
	$E_u^{(1)}(\text{TO})$	189	14	0.083
	$E_u^{(2)}(\text{LO})$	367	8.1	0.022
	$E_u^{(2)}(\text{TO})$	381.5	13	0.034
	$E_u^{(3)}(\text{LO})$	443.5	19.5	0.044
	$E_u^{(3)}(\text{TO})$	508	27	0.053
	$A_{2u}(\text{LO})$	796	60	0.075
	$E_u^{(1)}(\text{LO})$	831	65	0.078
ZrSiO ₄	value for each of the three $A_{2u}(\text{TO})$ modes (Ref. 9):	0.019.		
Al ₂ O ₃	average for LO and TO E_u -type modes (Ref. 6):	0.014		

hardening of the mode through fourth- and possibly sixth-order anharmonicity, the ratio evaluated at the frequency Ω_{TO} renormalized at 1550 K is still equal to 0.16. The shape of the Raman spectra^{2, 19} also indicates large anharmonicities in rutile.

Even if one admits the reliability of the fit of the A_{2u} -type mode spectrum at 1550 K, we have no direct evidence for the occurrence of the process represented in Fig. 1(c). It is, however, reasonable to suspect this process because this is the lowest-order one which can cause a dependence of the mode hardening on temperature that would be more than linear.

On the other hand, the large value of the anharmonic shift found for the $A_{2u}(\text{TO})$ mode at 1550 K, viz., 226 cm^{-1} , in comparison to the harmonic frequency $\omega_{\text{TO}} = 144 \text{ cm}^{-1}$, raises the problem of the consistency of the perturbation treatment to evaluate the self-energy shift. A limiting case of this problem is the utilization of the theory when the harmonic frequency is zero or purely imaginary, as is done by several authors.⁴ Actually the problem may be solved by incorporating in the unperturbed Hamiltonian the part of the anharmonic contribution which stabilizes the mode energy by employing a renormalization procedure. Treatments with³ and without^{10, 11} renormalization yield similar analytic expressions for the square of the observed frequency [Eq. (14)]. This is essentially due to the fact that the stabilizing anharmonic processes cause a purely real contribution to the phonon self-energy [Eqs. (7) and (9)].

Finally we want to point out that there is no

doubt that the studies of anharmonic coupling at low temperatures, as made by the majority of the authors, are necessary and give valuable information, but they should be completed by high-temperature studies that may permit the observation of higher-order processes. Furthermore the usefulness of reflectivity measurements at high temperature is to be emphasized because the

uncertainty on damping data is lowered with increasing temperature as a result of the lowering of the band top.

ACKNOWLEDGMENT

Numerical computations have been performed at the G. R. I., Orléans.

-
- ¹J. G. Traylor, H. G. Smith, R. M. Nicklow, and M. H. Wilkinson, *Phys. Rev. B* **3**, 3457 (1971).
- ²G. A. Samara and P. S. Peercy, *Phys. Rev. B* **7**, 1131 (1973).
- ³B. D. Silverman and R. J. Joseph, *Phys. Rev.* **129**, 2062 (1963).
- ⁴R. A. Cowley, *Philos. Mag.* **11**, 673 (1965); R. P. Lowndes and A. Rastoggi, *J. Phys. C* **6**, 932 (1973); G. A. Samara and B. Morosin, *Phys. Rev. B* **8**, 1256 (1973).
- ⁵F. Gervais, *Solid State Commun.* **13**, 1211 (1973).
- ⁶F. Gervais and B. Piriou, *J. Phys. C* **7**, 2374 (1974).
- ⁷W. G. Spitzer and D. A. Kleinman, *Phys. Rev.* **121**, 1324 (1961).
- ⁸F. Gervais, B. Piriou, and F. Cabannes, *Phys. Status Solidi B* **51**, 701 (1972); **55**, 143 (1973).
- ⁹F. Gervais, B. Piriou, and F. Cabannes, *J. Phys. Chem. Solids* **34**, 1785 (1973).
- ¹⁰A. A. Maradudin and A. E. Fein, *Phys. Rev.* **128**, 2589 (1962).
- ¹¹R. A. Cowley, *Adv. Phys.* **12**, 421 (1963).
- ¹²R. F. Wallis, I. P. Ipatova, and A. A. Maradudin, *Fiz. Tverd. Tela* **8**, 1064 (1966) [*Sov. Phys.-Solid State* **8**, 850 (1966)].
- ¹³L. E. Gurevich and I. P. Ipatova, *Zh. Eksp. Teor. Fiz.* **45**, 231 (1963) [*Sov. Phys.-JETP* **18**, 162 (1964)].
- ¹⁴R. A. Cowley, *J. Phys.* **26**, 659 (1965); A. D. Bruce, *J. Phys. C* **6**, 174 (1973).
- ¹⁵A. S. Barker, *Phys. Rev.* **136**, A1290 (1964); D. W. Berreman and F. C. Unterwald, *Phys. Rev.* **174**, 791 (1968); I. F. Chang, S. S. Mitra, J. N. Plendl, and L. C. Mansur, *Phys. Status Solidi* **28**, 663 (1968); R. P. Lowndes, *Phys. Rev. B* **1**, 2754 (1970); A. A. Kukharskii, *Solid State Commun.* **13**, 1761 (1973).
- ¹⁶F. Gervais, Thèse de Doctorat d'Etat, Appendix A (Orléans, 1973) (unpublished).
- ¹⁷W. G. Spitzer, R. C. Miller, D. A. Kleinman and L. E. Howarth, *Phys. Rev.* **126**, 1710 (1962).
- ¹⁸A. S. Barker and M. Tinkham, *J. Chem. Phys.* **38**, 2257 (1963).
- ¹⁹S. P. S. Porto, P. A. Fleury, and T. C. Damen, *Phys. Rev.* **154**, 522 (1967).
- ²⁰R. A. Parker, *Phys. Rev.* **124**, 1719 (1961).
- ²¹Instead of using the form $\Omega_j^2 = \omega^2(\vec{0}_j) + 2\omega(\vec{0}_j) [\Delta\omega(\vec{0}_j, \Omega_j, T) + \delta\omega_j(T)]$, where the frequency shift $\delta\omega_j$ due to thermal expansion is treated as an additional shift, one may introduce the quasiharmonic frequency $\omega(\vec{0}_j) + \delta\omega_j(T)$ that is renormalized by incorporating the pure-volume effect. Both procedures yield similar results because $\delta\omega_j$ is usually small.
- ²²C. Postmus, J. R. Ferraro, and S. S. Mitra, *Phys. Rev.* **174**, 983 (1968).
- ²³J. E. Eldridge and R. Howard, *Phys. Rev. B* **7**, 4652 (1973); J. E. Eldridge and K. A. Kembry, *Phys. Rev. B* **8**, 746 (1973).
- ²⁴P. G. Klemens, *Phys. Rev.* **148**, 845 (1966); K. Park, *Phys. Lett. A* **25**, 490 (1967); M. Askhin, J. H. Parker, and D. W. Feldman, *Solid State Commun.* **6**, 343 (1968); J. L. LaCombe and J. C. Irwin, *Solid State Commun.* **8**, 1427 (1970); T. Sakurai and T. Sato, *Phys. Rev. B* **4**, 583 (1971); I. F. Chang and S. S. Mitra, *Phys. Rev. B* **5**, 4094 (1972).